Integration of Highly Luminescent Lead Halide Perovskite Nanocrystals on Transparent Lead Halide Nanowire Waveguides through Morphological Transformation and Spontaneous Growth in Water

Tao Chen, Chong Wang, Xinxin Xing, Zhaojun Qin, Fan Qin, Yanan Wang, Md Kamrul Alam, Viktor G. Hadjiev, Guang Yang, Shuming Ye, Jie Yang, Rongfei Wang, Shuai Yue, Di Zhang, Zhongxia Shang, Francisco C. Robles-Hernandez, Hector A. Calderon Benavides, Haiyan Wang, Zhiming Wang, Jiming Bao**

Mr. T. Chen, Prof. C. Wang, S. M. Ye, Prof. J. Yang, Prof. R. F. Wang

National Center for International Research on Photoelectric and Energy Materials, School of Materials and Energy, Yunnan University, Kunming 650091, P. R. China

Email:cwang@ynu.edu.cn (C. Wang)

Dr. Z. J. Qin, Dr. X. Xing, Dr. F. Qin, Dr. Y. Wang, Dr. M. K. Alam, Dr. G. Yang, Dr. S. Yue, Prof. F. C. Robles-Hernandez, Prof. J. M. Bao

Department of Electrical and Computer Engineering, University of Houston, Houston, TX 77204, USA

Email:jbao@uh.edu (J. M. Bao)

Dr. Z. J. Qin, Dr. X. Xing, Dr. S. Yue, Prof. Z. M. Wang

Institute of Fundamental and Frontier Sciences, University of Electronic Science and Technology of China, Chengdu, Sichuan 610054, P. R. China

Prof. V. G. Hadjiev

Department of Mechanical Engineering, University of Houston, Houston, TX 77204, USA

Prof. J. M. Bao, Prof. V. G. Hadjiev

Texas Center for Superconductivity, University of Houston, Houston, TX 77204, USA

Dr. D. Zhang, Dr. Z. X. Shang, Prof. H. Y. Wang

School of Materials Engineering, Purdue University, West Lafayette, IN 47907, USA

Prof. F. C. Robles-Hernandez

Mechanical Engineering Technology, University of Houston, Houston, TX 77204, USA

Prof. H. A. Calderon Benavides

Instituto Politecnico Nacional, ESFM-IPN, UPALM, Departamento de Física, Mexico CDMX 07338, Mexico

Email: cwang@ynu.edu.cn (C. Wang), jbao@uh.edu (J. M. Bao)

Keywords: $CsPb_2Br_5$ nanowires, morphological transformation, nanowire waveguide integration, origin of luminescence, dissolution-recrystalization

Abstract

The integration of highly luminescent $CsPbBr_3$ quantum dots on nanowire waveguides has enormous potential applications in nanophotonics, optical sensing and quantum communications. On the other hand, $CsPb_2Br_5$ nanowires have also attracted a lot of attention due to their unique water stability and controversial luminescent property. Here we first report the growth of $CsPbBr_3$ nanocrystals on $CsPb_2Br_5$ nanowires by simply immersing $CsPbBr_3$ powder into pure water, $CsPbBr_{3-\gamma}X_\gamma$ (X = Cl, I) nanocrystals on $CsPb_2Br_{5-\gamma}X_\gamma$ nanowires are then synthesized for tunable light sources. Systematic structure and morphology studies, including in-situ monitoring, revealed that $CsPbBr_3$ powder was first converted to $CsPb_2Br_5$ microplatelets in water, followed by a morphological transformation from $CsPb_2Br_5$ microplatelets to nanowires, which is a kinetic dissolution-recrystallization process controlled by electrolytic dissociation and supersaturation of $CsPb_2Br_5$. $CsPbBr_3$ nanocrystals are spontaneously formed on $CsPb_2Br_5$ nanowires when nanowires are collected from the aqueous solution. Raman spectroscopy, combined photoluminescence and SEM imaging confirm that the bright emission originates from $CsPbBr_{3-\gamma}X_\gamma$ nanocrystals while $CsPb_2Br_{5-\gamma}X_\gamma$ nanowires are transparent waveguides. The intimate integration of nanoscale light sources with a nanowire waveguide is demonstrated through the observation of the wave guiding of light from nanocrystals and Fabry-Perot interference modes of the nanowire cavity.

1. Introduction

The integration of highly efficient fluorescent semiconductor nanocrystals or quantum dots with sub-micrometer waveguides is essential to the construction of photonic circuits for a wide range of applications in quantum information, optical communication and sensing.[1-6] Even although a few integration techniques have been developed over the years, for example, by physically placing nanocrystals to a waveguide,[4, 7, 8] chemically adsorption of nanocrystals on a waveguide,[9, 10] or using e-beam lithography[11, 12] to define and control relative position of nanocrystals and waveguides, the integration still remains challenging, since it involves precise manipulation of nanoscale objects. All-inorganic lead halide perovskite $CsPbBr_3$ quantum dots, because of their nearly 100% quantum efficiency, [13, 14] have emerged as an ideal candidate for non-classical light source.[10, 15-19] In particular, by integrating quantum dots with a waveguide, a single photon quantum source has been demonstrated.[20, 21]

Lead halide $CsPb_2Br_5$ perovskite has also attracted a lot of attention due to several reasons. First, unlike most lead halide perovskites, it is a water-stable wide band gap semiconductor. [22-27] Highly environment-stable lasers and light emitting diodes (LEDs) have been demonstrated by embedding perovskite nanocrystals such as $CsPbBr_3$ in transparent $CsPb_2Br_5$ matrix. [28-34] Second, as an intrinsic layered material, $CsPb_2Br_5$ can be synthesized in the form of 2-D platelets or 1-D nanowires, thus enabling more applications in nanophotonics. Finally, the origin of its bright green emission has been the center of heated debates and still requires further investigation.[22, 24, 35-41] In our previous work, we showed that $CsPbBr_3$ and $CsPbBr_{3-\gamma}X_\gamma$ (X = Cl, I) nanocrystals rather than Br vacancies are responsible for the tunable visible light emission in $CsPb_2Br_5$ platelets.[27] This discovery can be applied to emissive $CsPb_2Br_5$ and $CsPb_2Br_{5-\gamma}X_\gamma$ nanowires in principle, but a direct observation of $CsPbBr_3$ and $CsPbBr_{3-\gamma}X_\gamma$ nanocrystals has not been confirmed. [42, 43] As such, the origin of the visible emission remains yet to be determined.

In this work, we discovered a catalyst- and ligand-free method to synthesize $CsPb_2Br_5$ nanowires with or without decorated $CsPbBr_3$ nanocrystals. The nanowires were grown from the water solution of $CsPb_2Br_5$ platelets through a morphological transformation. Raman spectroscopy, same-spot photoluminescence imaging and scanning electron microscopy (SEM) confirmed that pure $CsPb_2Br_5$ nanowires have no green photoluminescence, and the decorated $CsPbBr_3$ nanocrystals are responsible for the green emissive $CsPb_2Br_5$ nanowires. Highly luminescent $CsPb_2Br_{5-\gamma}X_\gamma$ nanowires were also synthesized and the same conclusion as above was obtained. The integrated $CsPbBr_3$/$CsPb_2Br_5$ NC/NW exhibits a dual function as a waveguide-coupled light source and an optical Fabry-Perot cavity.

2. Results and Discussion

$CsPb_2Br_5$ platelets were first synthesized using the same method as before by simply dropping $CsPbBr_3$ micro-cubes (or powders) in a large quantity of pure water (>20 times in mass) in a flask or bottle at room temperature.[27] Similar water-triggered phase transformation has also been reported, [44-48] the transformation is due to a high solubility of $CsPbBr_3$ and a much lower solubility of $CsPb_2Br_5$ in water, $CsPb_2Br_5$ can be formed in seconds and become a white precipitate from the initial yellow $CsPbBr_3$ powders. This rapid structural conversion in water can be verified by in-situ Raman spectroscopy. **Figure 1**a shows the evolution of Raman spectrum when a small water droplet was added to $CsPbBr_3$ powders. The dissolution of $CsPbBr_3$ can be seen from the disappearance of its characteristic Raman peak at 310 cm^{-1}, and the emergence of $CsPb_2Br_5$ is manifested by the appearance of sharp Raman features below 100 cm^{-1} and 133 cm^{-1}.

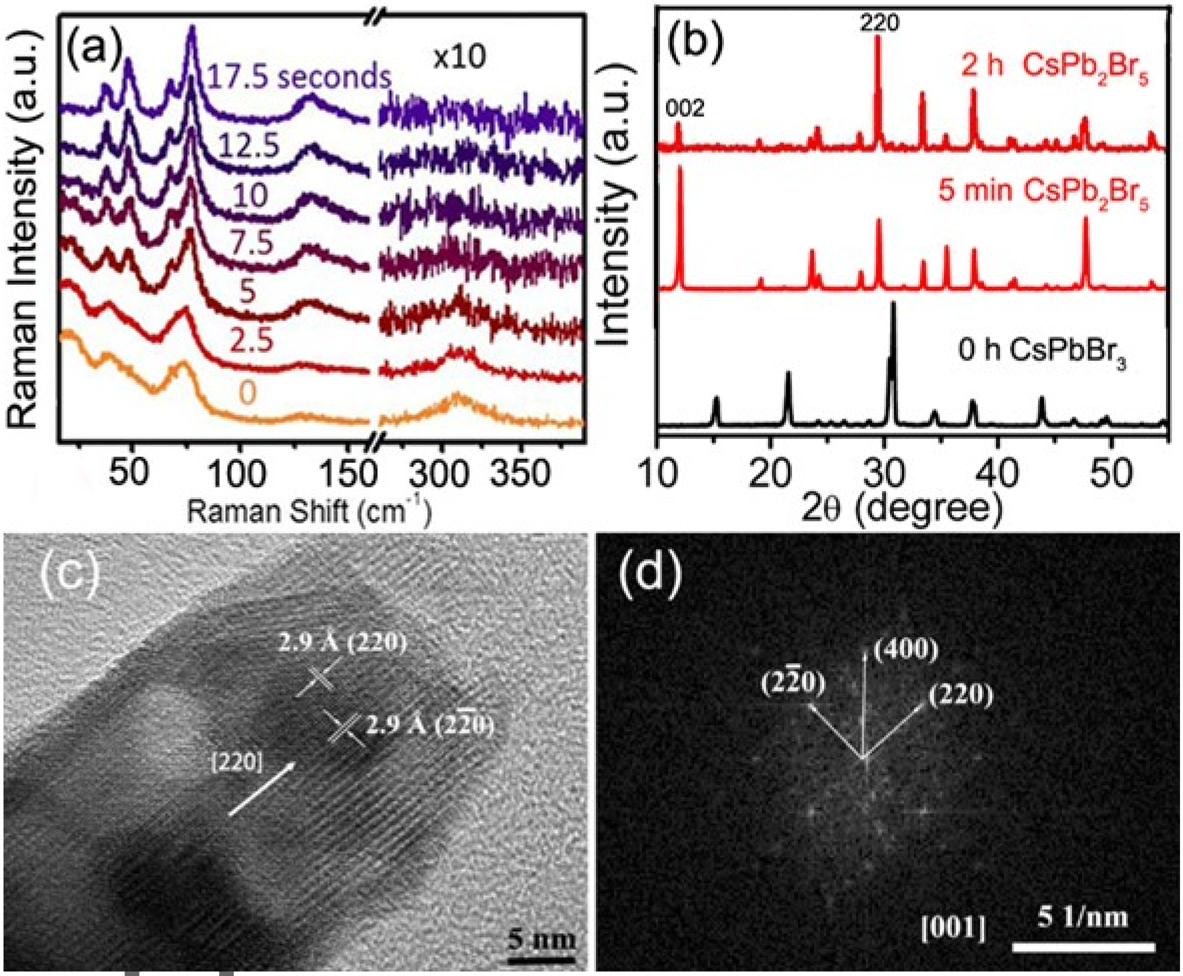

Figure 1. Raman, XRD and TEM characterizations of $CsPb_2Br_5$ nanowires. a) Evolution of Raman spectrum at room temperature when a droplet of water was added to $CsPbBr_3$ powder. b) XRD spectra of dry precipitates produced after immersing $CsPbBr_3$ powder in water with different immersion times. c) Representative HR-TEM image of a $CsPb_2Br_5$ nanowire and d) the corresponding fast Fourier transform (FFT) image.

To obtain $CsPb_2Br_5$ nanowires, we replaced the solution with fresh water while keeping the platelet precipitates at the bottom, then heated up the water with stiring on a hot plate. When the temperature reached 60 °C (in about 15 minutes), we stopped heating and stiring, let the solution cool down naturally. The formation of $CsPb_2Br_5$ nanowires can be revealed by a subtle change in X-ray diffraction (XRD) in **Figure 1**b: the relative intensity of (220) to (002) increases dramatically when the immersion time increases from 5 minutes to 2 hours, here the immersion time was counted from the exchange of water and beginning of the heating. The strong (002) peak in the 5-minute immersion sample is due to the intrinsic 2D layered structure of $CsPb_2Br_5$ platelets. The strong (220) peak in 2-hour sample indicates another preferred growth direction of $CsPb_2Br_5$ nanowires, which is confirmed by the high-resolution transmission electron microscopy (HR-TEM) image and corresponding fast Fourier transform (FFT) pattern shown in Figures 1c and 1d.

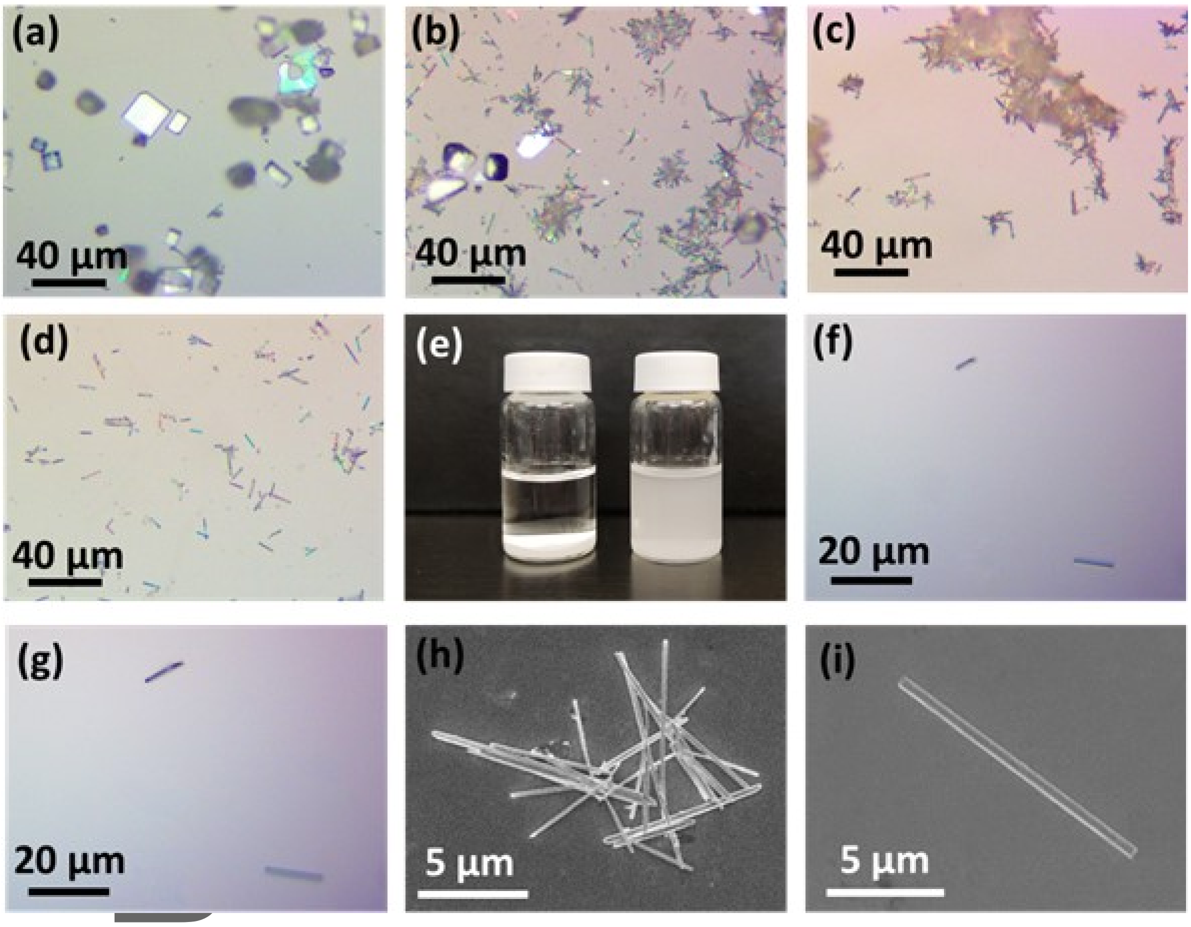

Figure 2. Optical and SEM images of $CsPb_2Br_5$ nanowires. a-d) Optical images of $CsPb_2Br_5$ after exchange of water for (a) 0 h, (b) 1 h, (c) 3 h and (d) 4 h. e) Pictures of water right after dropping off $CsPbBr_3$ (left) and after the conversion of $CsPb_2Br_5$ platelets to nanowires in 4 hours (right). f-g) In-situ observation of the growth of

$CsPb_2Br_5$ nanowires from $CsPb_2Br_5$ saturated water. Picture in (g) was taken about 10 minutes after the picture in (f). h-i) SEM images of $CsPb_2Br_5$ nanowires from (e).

To obtain a better understanding of $CsPb_2Br_5$ nanowire growth from $CsPb_2Br_5$ 2D platelets, we monitored morphology evolution of $CsPb_2Br_5$ precipitates with increasing immersion time. **Figures 2**a-d show representative optical images of $CsPb_2Br_5$ nanowires from exchange of water to 4 hours of immersion time. We observed that, first, unlike platelets, the growth of nanowires takes time. More nanowires will be formed as immersion time increases and a complete conversion to nanowires can also be achieved after 4 hours, which can be conveniently recognized by a milky white color of suspended $CsPb_2Br_5$ nanowires in **Figure 4**e. Second, these nanowires do not seem to grow from platelets since they are not attached to platelets. The latter observation is also confirmed by the in-situ observations of nanowire growth in solution. **Figures 2**f-g show optical images when a droplet of clean $CsPb_2Br_5$ water solution is left on a glass slide in air. As the droplet dries up, two nanowires appear and grow. A faster growth here is due to increased ion concentration as a result of quick evaporation of water in air. **Figures 2**h-i show SEM images of nanowires. It can be seen that nanowires are not tapered and can have diameter much less than 1 µm, but as optical pictures have also revealed, their lengths are not uniform.

Solution synthesis is a very common method to grow nanostructures. However, spontaneous morphological transformation in solution is rarely reported. [33, 49-51] If it happens, typically one type of nanostructures will grow from the other structures. For example, CeO_2 nanorods can grow on CeO_2 nano-octahedrons through the dissolution of the nano-octahedrons and recrystallization of the nanorods. [52] $CsPbBr_3$ nanowires are formed through oriented self-assembly of $CsPbBr_3$ nanocubes in solution. [53] Moreover, most anisotropic growth during the phase conversion takes place via solution method by adding complex ligands in the material synthetic process. [54, 55] In our case, nanowires and platelets are completely separated, and nanowires grow out of solution from Cs^{+}, Pb^{2+}, Br^{-} ions in water, which can be described as a dissolution-recrystallization during the transformation from $CsPb_2Br_5$ plates to nanowires. [33, 49-51, 56] According to recent work by Lai, *et al.*, [56] the crystallization morphology is controlled by supersaturation for a material that has a low electrolytic dissociation, such as $CsPb_2Br_5$ due to its low solubility in water. As such, a rapid recrystallization by dropping $CsPbBr_3$ powder in water will result in 2D $CsPb_2Br_5$ platelets, while 1D $CsPb_2Br_5$ nanowires will be formed due to slow cooling of $CsPb_2Br_5$ saturated aqueous solution.

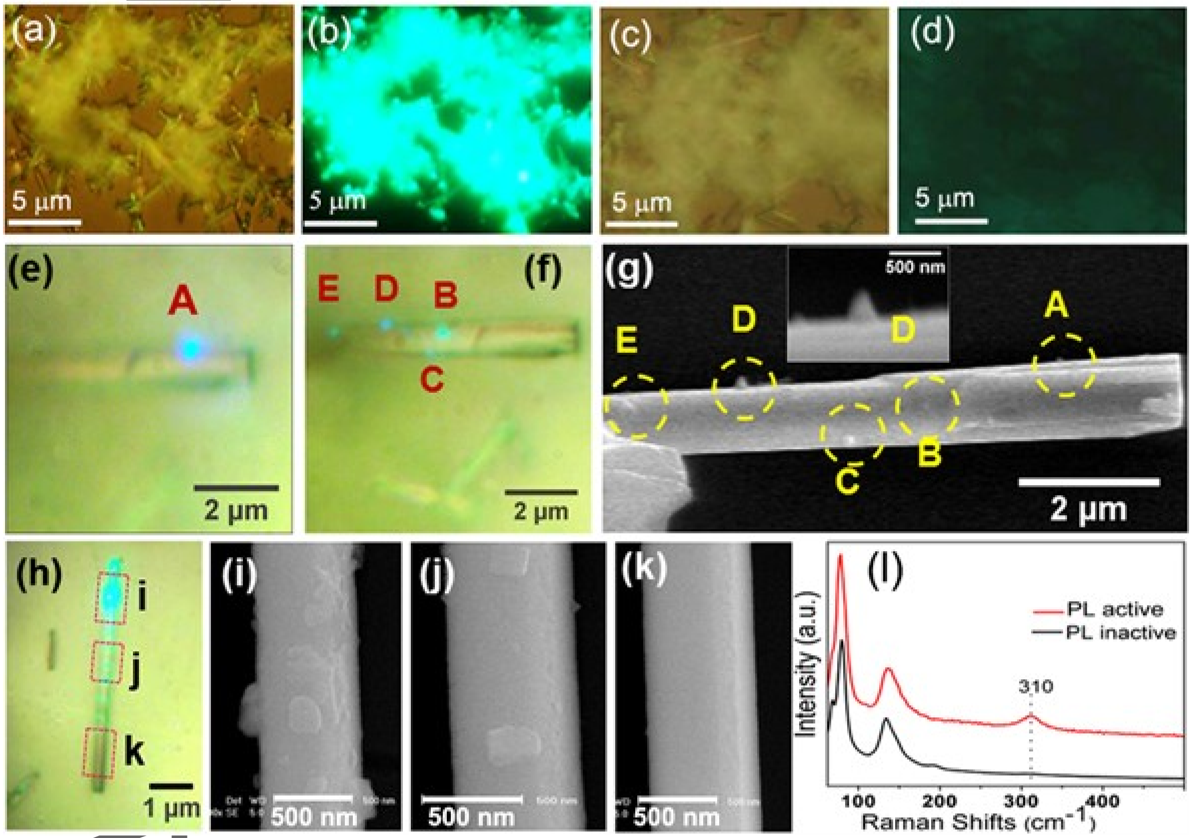

Figure 3. Optical, photoluminescence and SEM images, as well as Raman spectra of $CsPb_2Br_5$ nanowires. Optical images of $CsPb_2Br_5$ nanowires a) without and c) with cleaning. b, d) Corresponding photoluminescence images.

e-g, h-k) Photoluminescence and SEM images of two individual nanowires. l) Raman spectra of PL-active site and PL-inactive site of the same nanowire.

$CsPb_2Br_5$ nanowires were reported to exhibit strong green photoluminescence (PL). [42, 43] **This is confirmed in Figures 3a-b if we simply take the wires out of the water and let them dry. However, our previous work has shown that if the $CsPb_2Br_5$ platelets are carefully washed by water and ethanol, $CsPbBr_3$ nanocrystals cannot be formed on the surface of $CsPb_2Br_5$ platelets; subsequently, their green photoluminescence can be eliminated. To investigate the effect of post-synthesis drying on the optical property, we performed similar cleaning and drying steps. The results in Figures 3c-d confirmed our previous observations: the cleaned nanowires showed no PL emission. Following the same procedure as before, we compared Raman spectra of emissive and non-emissive nanowires, and we performed photoluminescence imaging and SEM imaging on the same nanowires to further verify $CsPbBr_3$ nanocrystals as the source of the green emission. SEM and PL images in Figures 3e-k confirm that overgrown nanocrystal bumps on nanowires are responsible for the green emission, and Raman spectra in Figure 3l confirms these bumps as $CsPbBr_3$ nanocrystals from their characteristic Raman line at 310 cm^{-1}.**

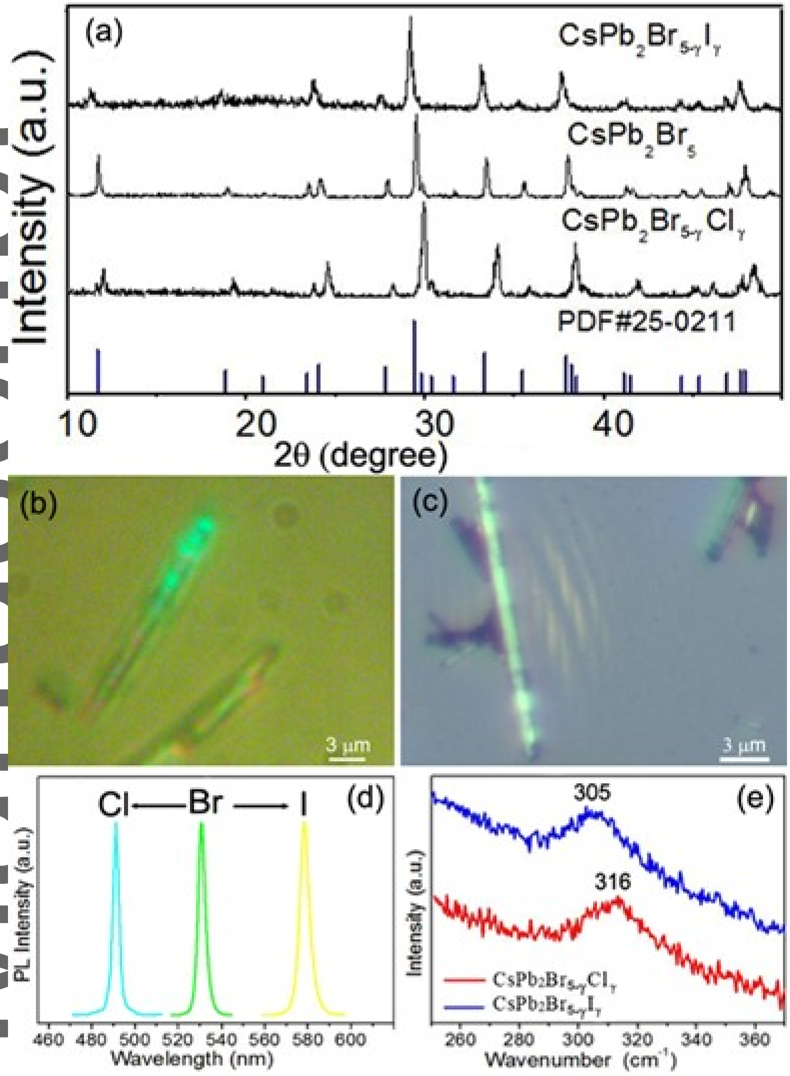

Figure 4. XRD, photoluminescence and Raman spectra of $CsPbBr_{3-\gamma}X_\gamma$ nanowires. a) XRD of $CsPb_2Br_5$, $CsPb_2Br_{5-\gamma}Cl_\gamma$ and $CsPb_2Br_{5-\gamma}I_\gamma$ nanowires. b-c) Photoluminescence images of b) $CsPb_2Br_{5-\gamma}Cl_\gamma$ and c) $CsPb_2Br_{5-\gamma}I_\gamma$. d) Representative PL spectra of emissive $CsPb_2Br_{5-\gamma}X_\gamma$. e) Raman spectra of PL-active $CsPb_2Br_{5-\gamma}Cl_\gamma$ and $CsPb_2Br_{5-\gamma}I_\gamma$ nanowires.

Having determined that $CsPbBr_3$ nanocrystals are responsible for the strong green emission in $CsPb_2Br_5$ nanowires, we believe that the previously observed emission in $CsPb_2Br_{5-\gamma}X_\gamma$ nanowires was also due to $CsPbBr_{3-\gamma}X_\gamma$. We can use two synthesis methods to prove this hypothesis. The first is to use the emissive $CsPb_2Br_5$ nanowires and ion exchange to partially replace Br^- with Cl^- or I^- in $CsPbBr_3/CsPb_2Br_5$, as we did for $CsPb_2Br_5$ platelets and ion exchange only took place on the surface of the $CsPb_2Br_5$ platelets. [27] The second approach is to synthesize $CsPbBr_{3-\gamma}X_\gamma$ first and then use water to convert $CsPbBr_{3-\gamma}X_\gamma$ to $CsPb_2Br_{5-\gamma}X_\gamma$. Here we use the latter method, the detailed procedures are described in Experimental Section. The successful incorporation of Cl or I into $CsPb_2Br_5$ crystal lattice can be seen from slightly shifted XRD peaks in **Figure 4**a. [42] The diffraction angles of $CsPb_2Br_{5-\gamma}I_\gamma$ ($CsPb_2Br_{5-\gamma}Cl_\gamma$) are reduced (increased) due to a larger (smaller) size of I (Cl) ions and subsequently a larger (smaller) lattice constant. This is different from the ion exchange using emissive $CsPb_2Br_5$ platelets, where no obvious change of lattice constant was observed. [27] We believe that ion exchange happened mainly to the surface $CsPbBr_3$ nanocrystals instead $CsPb_2Br_5$ platelets. [27] Following the same PL imaging and Raman spectroscopy technique, we can determine the origin of new luminescent centers. Specifically, PL images from individual nanowires in **Figures 4**b-c show that the emission does not come from the whole body of nanowires, but, instead from discrete bumps on the nanowires, which indicates that $CsPb_2Br_{5-\gamma}X_\gamma$ nanowires have no photoluminescence as $CsPb_2Br_5$ nanowires. Similar to $CsPb_2Br_5$ nanowires, PL of $CsPb_2Br_{5-\gamma}X_\gamma$ nanowires originated from the $CsPbBr_{3-\gamma}X_\gamma$ nanocrystals, which exhibit a blue or red spectral shift compared to that of $CsPbBr_3$, as shown in **Figure 4**d. [27] This conclusion is further supported by observations of Raman signature of $CsPbBr_{3-\gamma}X_\gamma$ nanocrystals shown in **Figure 4**e. [27]

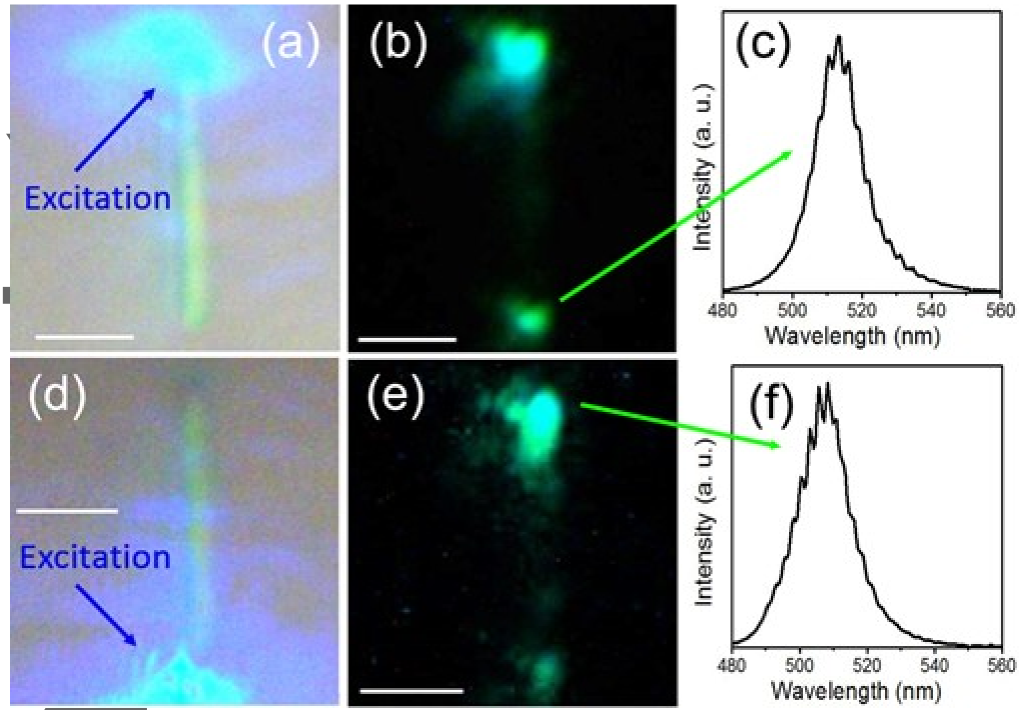

Figure 5. Optical coupling of $CsPbBr_3$ nanocrystals to $CsPb_2Br_5$ nanowire waveguide. a, d) Optical image of a $CsPb_2Br_5$ nanowire under white light illumination and 473-nm laser excitation from a) the top end and d) the bottom end. b, e) Corresponding photoluminescence images of (a) and (d) when the white light is turned off and laser is filtered out. c, f) Spectra of transmitted photoluminescence. Scale bar: 5 μm.

The integration of a nanoscale light emitter with a nanowire waveguide is the basic requirement for a nanophotonic circuit. Here we demonstrate two basic functions of $CsPbBr_3$/$CsPb_2Br_5$ nanocrystal/nanowire (NC/NW) as a waveguide and a light source. This can be done after we transfer a single $CsPbBr_3$/$CsPb_2Br_5$ NC/NW onto a CaF_2 substrate. **Figures 5**a-b show optical image of the NC/NW, where its top $CsPbBr_3$ end is excited by a laser beam. The coupling of excited green luminescence to the nanowire waveguide and its propagation to the bottom clean end can be seen from a visible but relatively weaker green spot. When the nanowire is excited from the bottom clean end, Figures 5d-e show a similar luminescence image: a stronger green emission on the top end and a relatively weak spot at the bottom end. This is because the top end has $CsPbBr_3$ nanocrystals. However, the way the $CsPbBr_3$ nanocrystals are excited is very different; in this case, it is the laser that couples to the nanowire, propagates to the top end, and excites the nanocrystals. Despite this different excitation method, Figures 5c, 5f and Figure S1 in the supporting information show that the green emission spectra exhibit well-known Fabry-Perot interference fringes, indicating a high nanowire optical cavity.

3. Conclusions

In summary, we discovered a platelet-to-nanowire morphological transformation and synthesized $CsPb_2Br_5$ nanowires in water. We have proved that both $CsPb_2Br_5$ and $CsPb_2Br_{5-\gamma}X_\gamma$ nanowires are non-emissive and can be used as optical waveguides. We have also shown that the decorated $CsPbBr_{3-\gamma}X_\gamma$ nanocrystals are responsible for the strong emission from $CsPb_2Br_{5-\gamma}X_\gamma$ nanowires. $CsPbBr_3$ and $CsPbBr_{3-\gamma}X_\gamma$ nanocrystals can spontaneously grow on the surface of $CsPb_2Br_{5-\gamma}X_\gamma$ nanowires. Although the location of $CsPbBr_{3-\gamma}X_\gamma$ nanocrystals on nanowires remains random, a precise position of nanocrystals can be achieved. For example, we can deposit a nanoscale droplet of $CsPbBr_{3-\gamma}X_\gamma$ aqueous solution on the nanowires using an AFM tip. [57, 58] The intimate integration of lead halide nanocrystals to lead halide nanowire waveguides provides us new opportunities for wider device applications of highly luminescent perovskite nanocrystals.

4. Experimental Section

The synthesis of $CsPbBr_3$ and $CsPbBr_{3-\gamma}X_\gamma$ (X=Cl or I) powder: $CsPbBr_3$ micro-cubes (or powders) were synthesized using a modified method by mixing 4 mmol $Pb(CH_3COO)_2{\cdot}3H_2O$ and 8 mmol CsBr in 10 mL 48% HBr solution (approximately 90 mmol) at room temperature and stirred for about 1 h.

$CsPbBr_{3-\gamma}X_\gamma$ (X=Cl or I) powder was synthesized by mixing 4 mmol $Pb(CH_3COO)_2{\cdot}3H_2O$, 2 mmol CsCl (or CsI) and 6 mmol CsBr in a solution containing 90 mmol HCl (or HI) and 270 mmol HBr.

XRD: XRD patterns of the samples were recorded on DX-2700BH X-ray diffractometer with a Cu Kα source.

SEM/TEM: SEM images were recorded on Nova Nano scanning electron microscope 450. TEM images were recorded on FEI Titan ETEM G2 80-300.

Raman/PL: Raman spectra and PL spectra were performed with Horiba LabSpec 6 which can measure Raman and PL on the same spot of a sample.

Supporting Information

Supporting Information is available from the Wiley Online or from the author.

Acknowledgements

T. C. and C.W. contributed equally to this work. C. W. would like to thank the financially support of the National Natural Science Foundation of China [No. 12164051 and No. 11564043], Joint Foundation of Provincial Science and Technology Department-Double First-class Construction of Yunnan University [No. 2019FY003016] and Young Top Talent Project of Yunnan Province [No. YNWR-QNBJ-2018-229]. T. C. thanks Advanced Analysis and Measurement Center of Yunnan University for the sample characterization service. J.M.B. acknowledges support from the Robert A. Welch Foundation (E-1728). The TEM work at Purdue was supported by the U.S. National Science Foundation (DMR-2016453 and DMR-1565822). Work at the Molecular Foundry (H. A. Calderon) was supported by the Office of Science, Office of Basic Energy Sciences, of the U.S. Department of Energy under Contract No. DE-AC02-05CH11231. J. Y. would like to thank the financially support of the National Natural Science Foundation of China [No. 62064013], the Application Basic Research Project of Yunnan Province [No. 2019FB130].

Conflict of Interest

The authors declare no conflict of interest.

Data Availability Statement

The data that support the findings of this study are available from the corresponding author upon reasonable request.

References

[1] M. A. Becker, R. Vaxenburg, G. Nedelcu, P. C. Sercel, A. Shabaev, M. J. Mehl, J. G. Michopoulos, S. G. Lambrakos, N. Bernstein, J. L. Lyons, T. Stoferle, R. F. Mahrt, M. V. Kovalenko, D. J. Norris, G. Raino, A. L. Efros, *Nature* **2018**, *553*, 189.

[2] Y. Cao, N. Wang, H. Tian, J. Guo, Y. Wei, H. Chen, Y. Miao, W. Zou, K. Pan, Y. He, H. Cao, Y. Ke, M. Xu, Y. Wang, M. Yang, K. Du, Z. Fu, D. Kong, D. Dai, Y. Jin, G. Li, H. Li, Q. Peng, J. Wang, W. Huang, *Nature* **2018**, *562*, 249.

[3] Y. Zhang, J. Liu, Z. Wang, Y. Xue, Q. Ou, L. Polavarapu, J. Zheng, X. Qi, Q. Bao, *Chem. Commun.* **2016**, *52*, 13637.

[4] A. V. Akimov, A. Mukherjee, C. L. Yu, D. E. Chang, A. S. Zibrov, P. R. Hemmer, H. Park, M. D. Lukin, *Nature* **2007**, *450*, 402.

[5] D. E. Chang, A. S. Sørensen, P. R. Hemmer, M. D. Lukin, *Phys. Rev. B* **2007**, *76*, 035420.

[6] A. Imamoglu, D. D. Awschalom, G. Burkard, D. P. DiVincenzo, D. Loss, M. Sherwin, A. Small, *Phys. Rev. Lett.* **1999,** *83*, 4204.

[7] F. Gu, H. Yu, P. Wang, Z. Yang, L. Tong, *ACS Nano* **2010**, *4*, 5332.

[8] K. Hennessy, A. Badolato, M. Winger, D. Gerace, M. Atature, S. Gulde, S. Falt, E. L. Hu, A. Imamoglu, *Nature* **2007**, *445*, 896.

[9] P. J. Cegielski, S. Neutzner, C. Porschatis, H. Lerch, J. Bolten, S. Suckow, A. R. S. Kandada, B. Chmielak, A. Petrozza, T. Wahlbrink, A. L. Giesecke, *Opt. Express* **2017**, *25*, 13199.

[10] J. Zhang, Y. H. Ye, X. Wang, P. Rochon, M. Xiao, *Phys. Rev. B* **2005,** *72*, 201306.

[11] Z. Hirboodvash, M. Khodami, N. R. Fong, E. Lisicka-Skrzek, A. Olivieri, H. Northfield, R. N. Tait, P. Berini, *Appl. Optics* **2019,** *58*, 2994.

[12] D. Chatzitheocharis, D. Ketzaki, C. Calo, C. Caillaud, K.Vyrsokinos, *Opt. Express* **2020,** *28*, 34219.

[13] O. H. Cheng, T. Qiao, M. Sheldon, D. H. Son, *Nanoscale* **2020,** *12*, 13113.

[14] K. Lin, J. Xing, L. N. Quan, F. P. G. de Arquer, X. Gong, J. Lu, L. Xie, W. Zhao, D. Zhang, C. Yan, W. Li, X. Liu, Y. Lu, J. Kirman, E. H. Sargent, Q. Xiong, Z. Wei, *Nature* **2018,** *562*, 245.

[15] D. D. Zhang, S. W. Eaton, Y. Yu, L. T. Dou, P. D. Yang, *J. Am. Chem. Soc.* **2015,** *137*, 9230.

[16] C. Fan, X. Xu, K. Yang, F. Jiang, S. Wang, Q. Zhang, *Adv. Mater.* **2018,** *30*, 1804707.

[17] Y. Meng, Z. Lai, F. Li, W. Wang, S.Yip, Q. Quan, X. Bu, F. Wang, Y. Bao, T. Hosomi, T. Takahashi, K. Nagashima, T. Yanagida, J. Lu, J. C. Ho, *ACS Nano* **2020,** *14*, 12749.

[18] Z. Gu, W. Sun, K. Wang, N. Zhang, C. Zhang, Q. Lyu, J. Li, S. Xiao, Q. Song, *J. Mater. Chem. A,* **2016**, *4*, 8015.

[19] S. Zou, G. Yang, T. Yang, D. Zhao, Z. Gan, W. Chen, H. Zhong, X. Wen, B. Jia, B. Zou, *J. Phys. Chem. Lett.* **2018,** *9*, 4878.

[20] H. Utzat, W. Sun, A. E. K. Kaplan, F. Krieg, M. Ginterseder, B. Spokoyny,N. D. Klein, K. E.Shulenberger, C. F. Perkinson, M. V. Kovalenko, M. G. Bawendi, *Science* **2019,** *363*, 1068.

[21] R. Uppu, H. T. Eriksen, H. Thyrrestrup, A. D. Ugurlu, Y. Wang, S. Scholz, A. D. Wieck, A. Ludwig, M. C. Lobl, R. J. Warburton, P. Lodahl, L. Midolo, *Nat. Commun.* **2020,** *11*, 3782.

[22] G. P. Li, H. Wang, Z. F. Zhu, Y. J. Chang, T. Zhang, Z. H. Song, Y. Jiang, *Chem. Commun.* **2016,** *52*, 11296.

[23] J. Yin, G. Zhang, X. Tao, *CrystEngComm* **2019,** *21*, 1352.

[24] Z. Zhang, Y. Zhu, W. Wang, W. Zheng, R. Lin, F. Huang, *J. Mater. Chem. C* **2018,** *6*, 446.

[25] I. Dursun, M. De Bastiani, B. Turedi, B. Alamer, A. Shkurenko, J. Yin, A. M. El-Zohry, I. Gereige, A. AlSaggaf, O. F. Mohammed, M. Eddaoudi, O. M. Bakr, *ChemSusChem* **2017,** *10*, 3746.

[26] P. Acharyya, P. Pal, P. K. Samanta, A. Sarkar, S. K. Pati, K. Biswas, *Nanoscale* **2019,** *11*, 4001.

[27] C. Wang, Y. Wang, X. Su, V. G. Hadjiev, S. Dai, Z. Qin, H. A. Calderon Benavides, Y. Ni, Q. Li, J. Jian, M. K. Alam, H. Wang, F. C. R. Hernandez, Y. Yao, S. Chen, Q. Yu, G. Feng, Z. Wang, J. Bao, *Adv. Mater.* **2019,** *31* 1902492.

[28] H. Huang, H. Lin, S. V. Kershaw, A. S. Susha,W. C. H. Choy, A. L. Rogach, *J. Phys. Chem. Lett.* **2016,** *7*, 4398.

[29] D. Zhang, Y. Yang, Y. Bekenstein, Y. Yu, N. A. Gibson, A. B. Wong, S. W.Eaton, N. Kornienko, Q. Kong, M. Lai, A. P. Alivisatos, S. R. Leone, P. Yang, *J. Am. Chem. Soc.* **2016,** *138*, 7236.

[30] L. Ruan, W. Shen, A. Wang, Q. Zhou, H. Zhang, Z. Deng, *Nanoscale* **2017,** *9*, 7252.

[31] J. Chen, J. Wang, X. Xu, J. Li, J. Song, S. Lan, S. Liu, B. Cai, B. Han, J. T. Precht, D. Ginger, H. Zeng, *Nat. Photon.* **2020,** *15*, 238.

[32] X. Zhang, B. Xu, J. Zhang, Y. Gao, Y. Zheng, K. Wang, X. W. Sun, *Adv. Funct. Mater.* **2016,** *26*, 4595.

[33] Z. Huang, B. Ma, H. Wang, N. Li, R. Liu, Z. Zhang, X. Zhang, J. Zhao, P. Zheng, Q. Wang, H. Zhang, *J. Phys. Chem. Lett.* **2020**, *11*, 6007.

[34] B. S. Zhu, H. Z. Li, J. Ge, H. D. Li, Y. C. Yin, K. H. Wang, C. Chen, J. S. Yao, Q. Zhang, H. B. Yao, *Nanoscale* **2018**, *10*, 19262.

[35] Z.-L. Yu, Y.-Q. Zhao, Q. Wan, B. Liu, J.-L. Yang, M.-Q. Cai, *J. Phys. Chem. C* **2020,** *124*, 23052.

[36] S. Cho, S. H. Yun, *Commun. Chem.* **2020,** *3,* 15.

[37] S. Lou, Z. Zhou, W. Gan, T. Xuan, Z. Bao, S. Si, L. Cao, H. Li, Z. Xia, J. Qiu, R.-S. Liu, J. Wang, *Green Chem.* **2020,** *22*, 5257.

[38] M. Cao, Y. Damji, C. Zhang, L. Wu, Q. Zhong, P. Li, D. Yang, Y. Xu, Q. Zhang, *Small Methods* **2020,** *4*, 2000303.

[39] K. Wang, L. Wu, L. Li, H. Yao, H. Qian, S. Yu, *Angew. Chem. Int. Ed.* **2016,** *55*, 8328.

[40] L. Zhang, K. Wang, Y. Lin, B. Zou, *J. Phys. Chem. Lett.* **2020,** *11*, 4693.

[41] Y. Q. Zhou, J. Xu, J. B. Liu, B. X. Liu, *J. Phys. Chem. Lett.* **2019,** *10*, 6118.

[42] L. Ruan, J. Lin, S. Shen, Z. Deng, *Nanoscale* **2018**, *10*, 7658.

[43] L. Ruan, W. Shen, A. Wang, A. Xiang, *J. Phys. Chem. Lett.* **2017**, *8*, 3853.

[44] B. Turedi, K. J. Lee, I. Dursun, B. Alamer, Z. Wu, E. Alarousu, O. F. Mohammed, N. Cho, O. M. Bakr, *J. Phys. Chem. C* **2018**, *122*, 14128.

[45] H. Dong, S. Kareem, X. Gong, J. Ruan, P. Gao, X. Zhou, X. Liu, X. Zhao, Y. Xie, *ACS Appl. Mater. Interfaces* **2021**, *13*, 23960.

[46] R.Wang, Z. Li, S. Li, P. Wang, J. Xiu, G. Wei, H. Liu, N. Jiang, Y. Liu, M. Zhong, J. Phys. Chem. C 2018, 122, 14128,.

[47] G. Maity, S. K. Pradhan, *J. Alloys Compd.* **2020**, *816*, 152612.

[48] L. Wu, H. Hu, Y. Xu. S. Jiang, M. Chen, Q. Zhong, D. Yang, Q. Liu, Y. Zhao, B. Sun, Q. Zhang, Y. Yin, *Nano Lett.* **2017**, *17*, 5799.

[49] L. Wang, G. Liu, L. Zou, D. Xue, *J. Alloys Compd.* **2010**, *493*, 471.

[50] Y. Sun, B. Mayers, T. Herricks, Y. Xia, *Nano Lett.* **2003**, *3*, 955.

[51] X. Xia, S. Xie, M. Liu, H. Peng, N. Lu, J. Wang, M. J. Kim, Y. Xia, *Proc. Natl. Acad. Sci.* **2013**,*110*, 6669.

[52] L. Yan, R. Yu, J. Chen, X. Xing, *Cryst. Growth & Des.* **2008**, *8*, 1474.

[53] Y. Tong, B. J. Bohn, E. Bladt, K. Wang, P. Müller-Buschbaum, S. Bals, A. S. Urban, L. Polavarapu, J. Feldmann, *Angew. Chem., Int. Ed.* **2017**, *56*, 13887.

[54] I. Pastoriza-Santos, L. M. Liz-Marzán, *Langmuir* **2002**, *18*, 2888.

[55] Z. A. Peng, X. Peng, *J. Am. Chem. Soc.* **2002**, *124*, 3343.

[56] W. H. Lai, Y. X. Wang, Y. Wang, M. Wu, J. Z. Wang, H. K. Liu, S. L. Chou, J. Chen, S. X. Dou, *Nat. Chem.* **2019**, *11*, 695.

[57] P. Galliker, J. Schneider, H. Eghlidi, S. Kress, V. Sandoghdar, D. Poulikakos, *Nat. Commun.* **2012**, *3*, 890.

[58] K. Kaisei, N. Satoh, K. Kobayashi, K. Matsushige, H. Yamada, *Nanotechnology*, **2011**, *22*, 175301.

Integration of Highly Luminescent Lead Halide Perovskite Nanocrystals on Transparent Lead Halide Nanowire Waveguides through Morphological Transformation and Spontaneous Growth in Water

Table of Contents

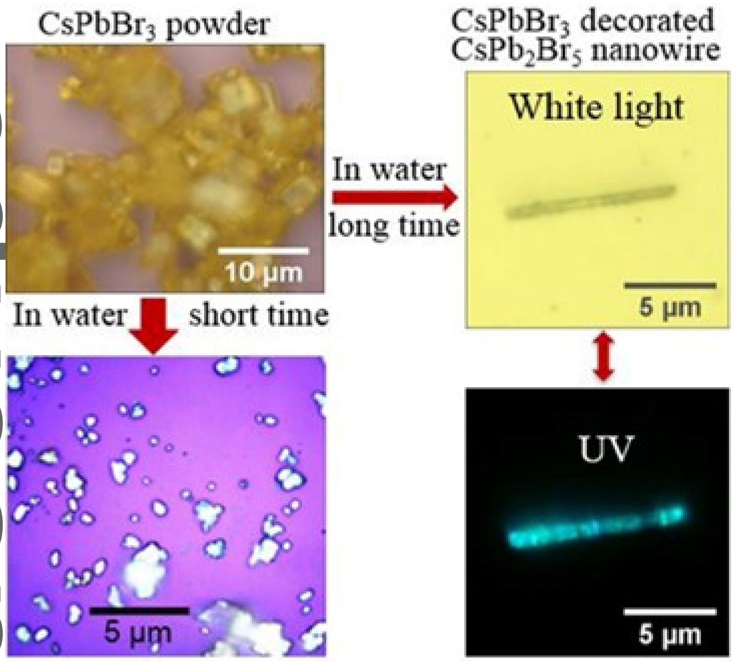

Morphological transformation from $CsPb_2Br_5$ platelets to nanowires in water is discovered and utilized to synthesize $CsPb_2Br_5$ nanowires from $CsPbBr_3$ powders. The integration of nanoscale light sources with nanowire waveguides through spontaneous growth of highly luminescent $CsPbBr_3$ nanocrystals on transparent $CsPb_2Br_5$ nanowires provides a new platform for optical sensing and quantum communications.